THE JOURNAL OF BIOLOGICAL CHEMISTRY Vol. 274, No. 53, Issue of December 31, pp. 37651–37657, 1999
Printed in U.S.A.

Contributions of the C-terminal Domain to the Control of P2X Receptor Desensitization*

(Received for publication, August 17, 1999, and in revised form, September 30, 1999)

Taka-aki Koshimizu, Miharu Koshimizu, and Stanko S. Stojilkovic‡

From the Endocrinology and Reproduction Research Branch, NICHD, National Institutes of Health, Bethesda, Maryland 20892

The P2X purinergic receptor channels (P2XRs) differ among themselves with respect to the rates of desensitization during prolonged agonist stimulation. Here we studied the desensitization of recombinant channels by monitoring the changes in intracellular free Ca^{2+} concentration in cells stimulated with ATP, the native and common agonist for all P2XRs. The focus in our investigations was on the relevance of the P2XR C terminus in controlling receptor desensitization. When expressed in GT1 cells, the P2XRs desensitized with rates characteristic to each receptor subtype: $P2X_1R$ = $P2X_3R$ > $P2X_{2b}R$ > $P2X_4R$ > $P2X_{2a}R$ > $P2X_7R$. A slow desensitizing pattern of $P2X_{2a}R$ was mimicked partially by $P2X_3R$ and fully by $P2X_4R$ when the six-amino acid sequences of these channels located in the cytoplasmic C terminus were substituted with the corresponding arginine 371 to proline 376 sequence of $P2X_{2a}R$. Changing the total net charge in the six amino acids of $P2X_4R$ to a more positive direction also slowed the receptor desensitization. On the other hand, substitution of arginine 371-proline 376 sequence of $P2X_{2a}R$ with the corresponding sequences of $P2X_1R$, $P2X_3R$, and $P2X_4R$ increased the rate of receptor desensitization. Furthermore, heterologous polymerization of wild-type $P2X_{2a}R$ and mutant $P2X_3R$ having the C-terminal six amino acids of $P2X_{2a}R$ at its analogous position resulted in a functional channel whose desensitization was significantly delayed. These results suggest that composition of the C-terminal six-amino acid sequence and its electrostatic force influence the rate of receptor desensitization.

ATP-gated receptor channels (P2XRs)[1] are expressed in a number of tissues where they are involved in regulation of a wide variety of cellular functions, including central and peripheral neurotransmission, smooth muscle contraction, platelet activation, and hormone secretion (1–3). The regulation of these functions by the activated P2XRs requires or is susceptible to local and/or global changes in intracellular Ca^{2+} concentration ($[Ca^{2+}]_i$) (3). Binding of extracellular ATP to P2XRs is associated with a rise in $[Ca^{2+}]_i$, which is mediated by Ca^{2+} influx through these channels as well as by depolarization of cells and activation of voltage-gated Ca^{2+} channels. The pattern of $[Ca^{2+}]_i$ signaling by native P2XRs is highly variable, depending on the cell type examined (3). In contrast to other Ca^{2+}-conducting channels, however, the relevant structural base of the P2XRs contributing to the control of $[Ca^{2+}]_i$ signaling function has not been completely elucidated.

Using molecular cloning techniques, seven subunits of P2XRs have been obtained so far and are named $P2X_1R$ to $P2X_7R$ (4–10). They can form Ca^{2+}-permeable pores through homo- and heteropolymerization (11, 12). Each subunit is proposed to have two putative transmembrane helices connected with a large extracellular loop, and both the N and C termini are located in the cytoplasm. From their N termini to the second transmembrane domain, the cloned subunits exhibit a relatively high level of amino acid (aa) sequence homology compared with their C termini, which are variable in lengths and show no apparent sequence homology except for the proximal region near the second transmembrane domain (1). During continuous exposure to agonist, current signals generated by recombinant P2XRs are desensitized gradually, an action that should effectively attenuate or terminate direct and indirect Ca^{2+} influx.

Based on the observed differences in their current desensitization kinetics, recombinant P2XRs are generally divided into two groups: the rapidly desensitizing ($P2X_1R$ and $P2X_3R$) and the slowly desensitizing ($P2X_2R$, $P2X_4R$, $P2X_5R$, $P2X_6R$, and $P2X_7R$) (3). Experiments with chimera subunits composed of $P2X_2R$ and $P2X_1R$ or $P2X_3R$ subunits suggested that the rapid desensitization requires interactions between two transmembrane domains of receptor subunits (13). A large C terminus of $P2X_7R$ has also been suggested to account for the nondesensitizing pattern of these channels during repetitive stimulation (10). Recently, a new view of P2XR desensitization has emerged; the C-terminal splice variant of $P2X_2R$, termed $P2X_{2b}R$ or $P2X_{2-2}R$, was found to lack a stretch of 69 aa and to desensitize faster than the full-length $P2X_2R$, termed $P2X_{2a}R$ (14–16). Amino acids responsible for such a functional difference between the spliced and full-length channels are localized to the initial six residues (Arg^{371}-Pro^{376}) within the spliced segment (17).

Here, we examined the importance of the C-terminal 6-aa sequences of P2XRs, which correspond to Arg^{371}-Pro^{376} of $P2X_{2a}R$ (Fig. 1), to the desensitization pattern of these channels. For this purpose, P2XRs and their mutants were expressed in GT1 immortalized neurons, and the impact of receptor desensitization on the pattern of $[Ca^{2+}]_i$ signaling was analyzed by monitoring single cell $[Ca^{2+}]_i$. These cells are excitable and express two types of voltage-gated calcium channels, T- and L-type (18). On the other hand, neither P2XRs nor Ca^{2+}-mobilizing P2Y receptors are native for these cells (16). Our results indicate that the pattern of receptor desensitization is unique for each homo- and heteropolymeric channel and that the structural differences in the C-terminal small region in part account for such variety of responses.

* The costs of publication of this article were defrayed in part by the payment of page charges. This article must therefore be hereby marked "*advertisement*" in accordance with 18 U.S.C. Section 1734 solely to indicate this fact.

‡ To whom correspondence should be addressed: Section on Cellular Signaling, ERRB/NICHD, Bldg. 49, Rm. 6A-36, 49 Convent Dr., Bethesda, MD 20892-4510. Tel.: 301-496-1638; Fax: 301-594-7031; E-mail: stankos@helix.nih.gov.

[1] The abbreviations used are: P2XR, ATP-gated receptor channels; aa, amino acid(s); PCR, polymerase chain reaction; AMP-CPP, adenosine 5′-(α,β-methylene)triphosphate.

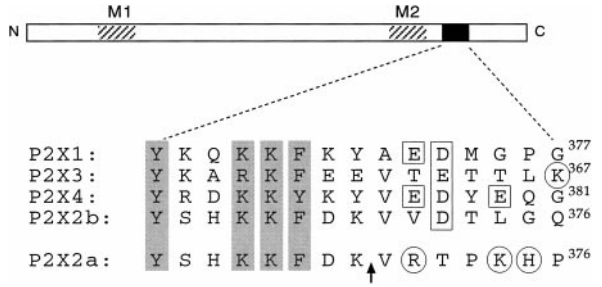

FIG. 1. **Schematic representation of the P2XR with two putative transmembrane domain model and amino acid sequences of the proximal C termini.** *Shading* indicates conserved residues. In the terminal six-amino acid segments shown, negatively charged residues are indicated by *squares*, and positively charged residues are indicated by *circles*. The *arrow* indicates the beginning of the spliced site in $P2X_{2a}R$ C terminus. M1 and M2 indicate the transmembrane domains 1 and 2, and N and C indicate the N and C termini, respectively.

EXPERIMENTAL PROCEDURES

Expression Constructs and Site-directed Mutagenesis—Protein coding sequences for rat $P2X_1R$ (4), $P2X_3R$ (6), $P2X_4R$ (19), $P2X_6R$ (9), and $P2X_7R$ (10) were obtained by PCR with reverse-transcribed mRNA from heart ($P2X_1R$), pituitary ($P2X_3R$), and brain ($P2X_4R$, $P2X_6R$, and $P2X_7R$), respectively. Total RNA was isolated using Trizol™ reagent (Life Technologies, Inc) and was treated with DNase I at 37 °C for 30 min. After heat inactivation of DNase I by incubating it at 70 °C for 15 min, first-strand cDNA was synthesized from 5 μg of total RNA by Superscript II reverse transcriptase and oligo$(dT)_{12-18}$ primers in a reaction volume of 20 μl. The resulting single-strand cDNA (1 μl) was then used as a template in 25 μl of PCR containing 2 mM each of four deoxynucleoside triphosphates, 50 mM KCl, 10 mM Tris-HCl (pH 8.3), 2 mM $MgCl_2$, and 0.5 units of Ex *Taq* polymerase (PanVera Corp., Madison WI). Primer annealing sites were selected from 3′- and 5′-untranslated regions and had the following sequences: X1 sense, 5′-GGCCGTGTGGGGTGTTCATCTCT-3′; X1 antisense, 5′-TCCAAAGTCTTGCCTGTCTTCAT-3′; X3 sense, 5′-TAAGTGGCTGTGAGCAGTTTCTC-3′; X3 antisense, 5′-GGAAGCATTGCCTATCTGTTGAA-3′; X4 sense, 5′-TGGCGAGGGGACCCACAGTGTC-3′; X4 antisense, 5′-GAGCCGGGCTCCAACAAGATGT-3′; X6 sense, 5′-ACTGGGACCATGGCTTCTGC-3′; X6 antisense, 5′-AACCACTCCTGAGACACCTG-3′; X7 sense, 5′-CCAGGTCCCGCCGAAACAGAGT-3′; and X7 antisense, 5′-GGCCTAACAATCCCTTCAACAC-3′. In the X6 sense primer, a point mutation (underlined) was introduced to obtain optimum translation efficiency (20). PCR products were separated on a 1% agarose gel, recovered, and subcloned into pBluescript II vector (Stratagene, La Jolla, CA) at its *Hinc*II site pretreated with 2′-deoxythymidine and *Taq* DNA polymerase (Life Technologies, Inc.). Sequences of subcloned inserts were verified in both strands with vector- and insert-specific primers using T7 sequenase (U. S. Biochemical Corp.). Confirmed inserts as well as cDNAs for $P2X_{2a}R$, $P2X_{2b}R$, and $P2X_5R$ (16) were transferred to pcDNA 3.1 (Invitrogen, Carlsbad, CA) at the *Xho*I/*Not*I site for mammalian expression.

All C-terminal mutants were made by a PCR-based overlap extension method (21) using the wild-type receptor cDNA as a template. Entire PCR fragments carrying mutations were subcloned into pBluescript II, sequenced, and transferred to C termini of the wild-type expression constructs using the following restriction sites: *Cla*I/*Hin*dIII, *Bsp*EI/*Hin*dIII, *Pst*I/*Hin*dIII, and *Sma*I for $P2X_{2a}R$, $P2X_3R$, $P2X_4R$, and $P2X_7R$ mutants, respectively. All restriction enzymes were obtained from New England Biolabs (Beverly, MA). The full-length $P2X_3R$ and its chimera mutant with $P2X_{2a}R$ were transferred from pBluescript to a bicistronic enhanced fluorescent protein vector, pIRES2-EGFP (CLONTECH, Palo Alto, CA), at its *Xho*I/*Eco*RI site, generating pIRES/$P2XR_3$ and pIRES/$P2X_3/X_{2a}R$, respectively.

Cell Cultures and Transfection—GT1 cells were cultured in Dulbecco's modified Eagle's medium/Ham's F-12 (1:1) containing 10% (v/v) fetal bovine serum, 100 μg/ml streptomycin, and 100 units/ml penicillin. Procedures for transient transfection in GT1 cells were performed as described (17) with minor modifications. Briefly, cells were plated on coverslips coated with poly-L-lysine at a density of 0.5–1.0 $\times$ 10^5 cell/35-mm dish and allowed to grow for 24 h. On the day of transfection, the total amount of 1.2 μg of expression constructs encoding wild-type or mutant P2XRs was mixed with 8 μl of cationic lipid, LipofectAMINE™, in 1.2 ml of reduced serum medium, Opti-MEM (Life Technologies, Inc.) for 15 min at ambient temperature. The DNA mixture was then applied to cells for 3–5 h and replaced by normal culture medium. The cells were subjected to experiments 24–48 h after the transfection. For co-transfection experiments, a ratio of 1:2 DNA for $P2X_{2a}R$ and pIRES constructs was used, keeping the total DNA amount same as above.

$[Ca^{2+}]_i$ Measurements—For single cell $[Ca^{2+}]_i$ measurements, cells were incubated at 37 °C for 60 min with 1 μM fura-2 AM in phenol red- and ATP-free Dulbecco's modified Eagle's medium. The cells were subsequently washed with assay buffer containing 137 mM NaCl, 5 mM KCl, 1.2 mM $CaCl_2$, 1 mM $MgCl_2$, 10 mM HEPES (pH 7.4), and 10 mM glucose and kept for at least 30 min in this medium before measurements. Apyrase (grade I) was purchased from Sigma and used at 20 μg/ml throughout the incubation process indicated. Coverslips with cells were mounted on the stage of an Axiovert 135 microscope (Carl Zeiss, Oberkochen, Germany) attached to the Attofluor digital fluorescence microscopy system (Atto Instruments, Rockville, MD). $[Ca^{2+}]_i$ responses were examined under a 40× oil immersion objective during exposure to alternating 340- and 380-nm light beams, and the intensity of light emission at 520 nm was measured. The ratio of light intensities, F_{340}/F_{380}, which reflects changes in $[Ca^{2+}]_i$, was simultaneously followed in several single cells. Cells expressing fluorescence protein were optically detected by an emission signal at 520 nm when excited by 488-nm ultraviolet light and were not detectable by 340- or 380-nm excitations. We thus considered the emission signal from fluorescence protein by 340- or 380-nm excitations within our background level. In co-transfection experiments of $P2X_{2a}R$ cDNA and pIRES vectors, about 75% of fluorescent protein-positive cells responded to 100 μM ATP stimulation and were considered to be co-transfected. Lower co-transfection efficiency below this level tended to show small response, and such experiments were excluded from further analysis.

Calculations—Since transfection efficiencies and expression levels of recombinant receptors were variable among the cells, only cells showing the peak $[Ca^{2+}]_i$ amplitude of more than 1.0 in the F_{340}/F_{380} ratio scale were further used for evaluating the desensitization rates. The time course of $[Ca^{2+}]_i$ response to ATP was fitted to one or two exponential functions using SigmaPlot 5.0 (Jandel Scientific software, San Rafael, CA) with the tolerance value set at 10^{-5}. Significant differences were determined by either Student's t test or one-way analysis variance (ANOVA) followed by Scheffe's test, if applicable; $p < 0.05$ was considered as significantly different.

RESULTS

Desensitization Pattern of Homopolymeric P2XRs—Our previous results have shown that GT1 cells are a suitable cell model for analyzing the $P2X_{2aR}$ and $P2X_{2bR}$ desensitization by single cell $[Ca^{2+}]_i$ measurements (16, 17). Here we show that all members of P2XRs, when expressed individually, responded to 100 μM ATP with a significant rise in $[Ca^{2+}]_i$. In cells transfected with $P2X_1R$ or $P2X_3R$ cDNA, however, preincubation of cultures with apyrase, an ectonucleotidase that degrades ATP, was necessary to detect any appreciable $[Ca^{2+}]_i$ change. Preincubation of $P2X_{2a}R$-expressing cells with this enzyme did not alter the pattern of $[Ca^{2+}]_i$ response compared with that observed in controls (not shown).

The averaged peak $[Ca^{2+}]_i$ amplitudes induced by supramaximal concentrations of ATP apparently differed among P2XRs. When stimulated with 100 μM ATP, the amplitudes of $[Ca^{2+}]_i$ were comparable among cells expressing $P2X_{2a}R$, $P2X_{2b}R$, and $P2X_4R$, whereas 500 μM ATP was required to reach the comparable $[Ca^{2+}]_i$ response in $P2X_7R$-transfected cells. The peak $[Ca^{2+}]_i$ responses caused by activated $P2X_1R$ and $P2X_3R$ with 100 μM ATP were about one-third those observed in cultures expressing $P2X_{2a}R$. A small fraction (less than 10%) of cells transfected with $P2X_5R$ or $P2X_6R$ cDNAs also responded to 100–500 μM ATP but with the amplitude of $[Ca^{2+}]_i$ responses about one-fifth that seen in the $P2X_{2a}R$. Because of such low and variable $[Ca^{2+}]_i$ responses, $P2X_5R$ and $P2X_6R$ were not employed in further studies.

As illustrated in Fig. 2*A*, the receptors also differed in their capacities to sustain $[Ca^{2+}]_i$ signaling during continuous stimulation with ATP. The $P2X_1R$- and $P2X_3R$-expressing cells completely terminated $[Ca^{2+}]_i$ signaling within 1–2 min of stimulation with 100 μM ATP. The $[Ca^{2+}]_i$ responses caused by

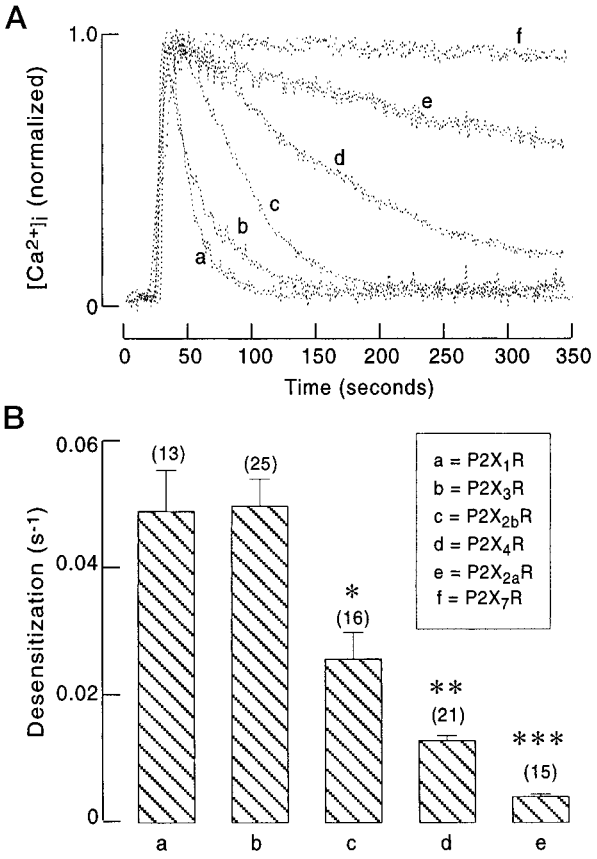

FIG. 2. **Pattern of calcium signaling by homopolymeric P2XRs transiently expressed in GT1 cells.** *A*, representative tracings of ATP-induced $[Ca^{2+}]_i$ signals, with normalized amplitudes of $[Ca^{2+}]_i$ responses (*y* axes). The $P2X_7R$-expressing cells were stimulated with 500 μM ATP, whereas the other receptor-expressing cells were stimulated with 100 μM ATP. *B*, the calculated desensitization rates were derived from single exponential fittings. The *bars* shown are the means ± S.E. derived from the *number* of trials indicated above the bars. *, $p < 0.05$ between $P2X_1R$/$P2X_3R$ and $P2X_{2b}R$; **, $p < 0.05$ between $P2X_{2b}R$ and $P2X_4R$; and ***, $p < 0.05$ between $P2X_4R$ and $P2X_{2a}R$.

activation of $P2X_{2b}R$ and $P2X_4R$ showed a relatively slow decrease compared with those generated by the $P2X_1R$ and $P2X_3R$. In contrast, $P2X_{2a}R$- and $P2X_7R$-expressing cells induced long-lasting $[Ca^{2+}]_i$ signals. The $P2X_{2a}R$-induced $[Ca^{2+}]_i$ signals usually decreased to one-third of maximum response, and this steady-state plateau level was reached within 10 min of stimulation. The $P2X_7R$-expressing cells showed no obvious decline in $[Ca^{2+}]_i$ response for more than 10 min. In all cases, except for $P2X_7R$, single exponential functions were sufficient to describe the decline rates of $[Ca^{2+}]_i$ responses. The mean values of calculated rate constants are shown in Fig. 2*B*. The rank order of desensitization rates derived from these data ($P2X_1R = P2X_3R > P2X_{2b}R > P2X_4R > P2X_{2a}R > P2X_7R$) was highly comparable with that observed in current measurements (22), confirming the validity of single cell $[Ca^{2+}]_i$ measurements as a method for comparative evaluation of receptor desensitization.

Role of a C-terminal 6-aa Sequence in Receptor Desensitization—Recently, we found that the Arg^{371}-Pro^{376} sequence, located in the cytoplasmic region of $P2X_{2a}R$, is necessary for the slow desensitizing pattern of these receptors (17). As shown in Fig. 1, this 6-aa region is located near the second putative transmembrane domain, and the C-terminal difference in amino acid sequences among the members of P2XRs starts from this region. To study the possible role of structural diversity of this region in the control of receptor desensitization, the

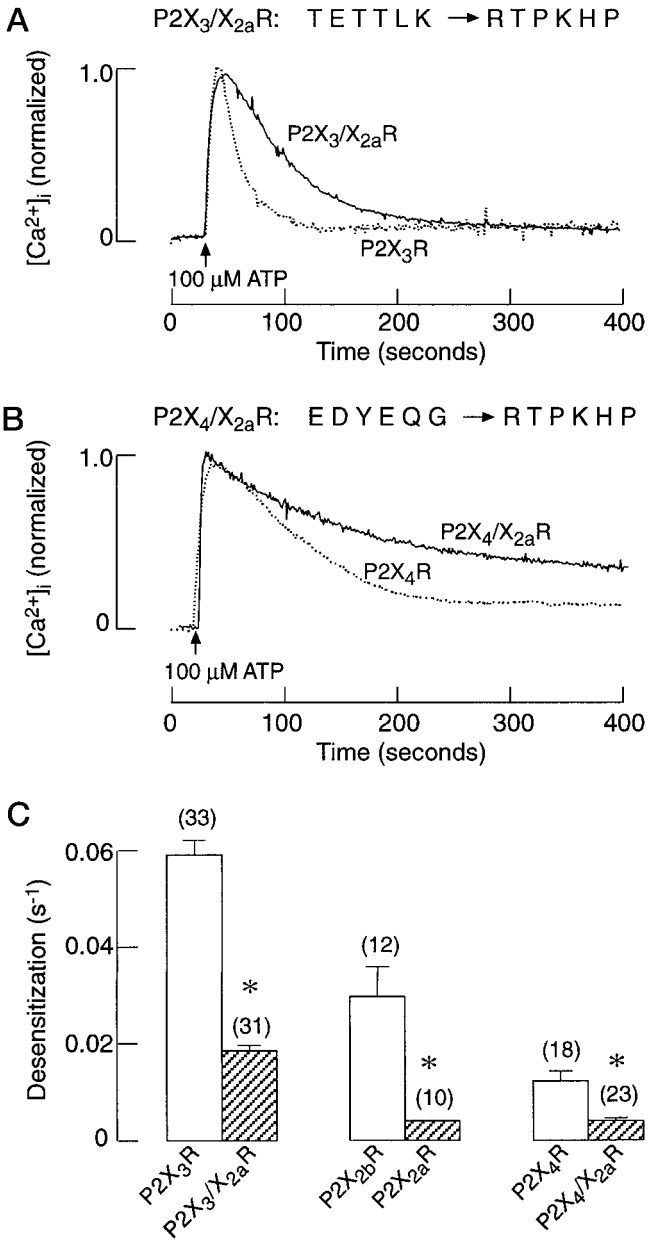

FIG. 3. **Calcium signaling in GT1 cells expressing chimeric P2XRs bearing the Arg^{371}-Pro^{376} sequence of $P2X_{2a}R$.** *A*, pattern of ATP-induced calcium signals in wild-type $P2X_3R$ and mutant $P2X_3/X_{2a}R$. Cells were stimulated with 100 μM ATP in the presence of 20 μg/ml apyrase. *B*, pattern of Ca^{2+} signaling in cells expressing wild-type $P2X_4R$ and mutant $P2X_4/X_{2a}R$. The tracings shown in *A* and *B* are computer-derived means from 8–10 single cell recordings. *C*, comparison of the desensitization rates for native and mutant receptors with or without Arg^{371}-Pro^{376} sequence. The *bars* shown are mean ± S.E. derived from the *number* of trials indicated above the bars. *$p < 0.05$ or higher among pairs.

Arg^{371}-Pro^{376} sequence of $P2X_{2a}R$ was introduced to $P2X_3R$ and $P2X_4R$ instead the native Thr^{362}-Lys^{367} and Glu^{376}-Gly^{381} sequences, respectively. Such C-terminal chimeric subunits were termed $P2X_3/X_{2a}R$ and $P2X_4/X_{2a}R$ (Figs. 1 and 3). Cells expressing the $P2X_3/X_{2a}R$ mutant responded to 100 μM ATP with an apparent delay in desensitization of $[Ca^{2+}]_i$ signals compared with the wild-type $P2X_3R$ (Fig. 3*A*). Furthermore, the averaged spike $[Ca^{2+}]_i$ amplitude was significantly higher in cells expressing $P2X_3/X_{2a}R$ than in cells expressing $P2X_3R$ (F_{340}/F_{380}: 1.6 ± 0.1 (n = 31) *versus* 2 ± 0.05 (n = 34), respectively). As seen in wild-type $P2X_3R$, the addition of apyrase to the bath solution was necessary to detect the $[Ca^{2+}]_i$ change in

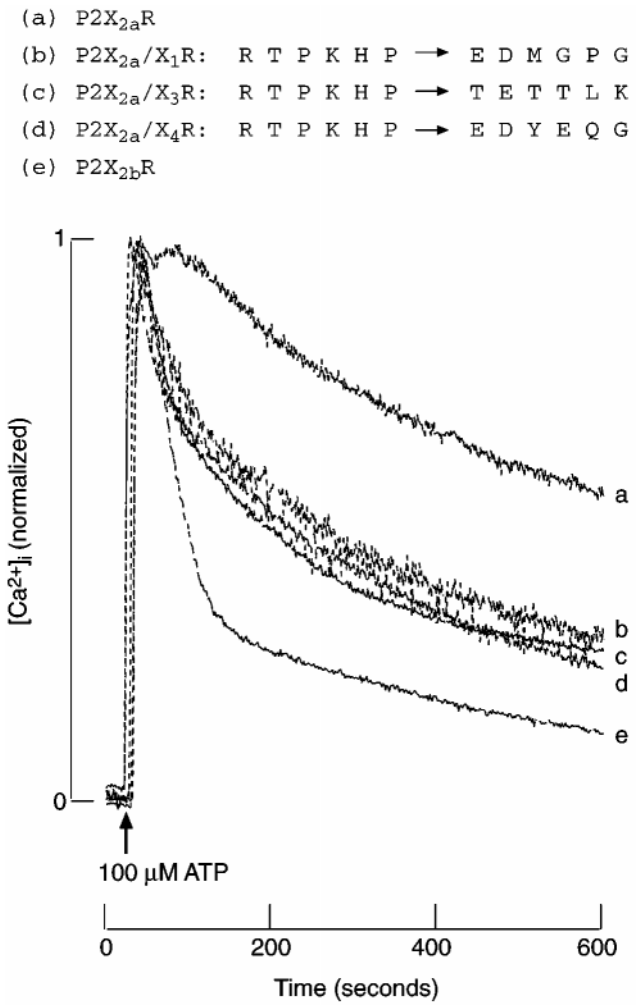

FIG. 4. **Calcium signaling in GT1 cells expressing wild-type and mutant $P2X_{2a}R$.** The *tracings* shown are means from at least 18 recordings. The time constants are shown in Table I.

$P2X_3/X_{2a}R$-expressing cells, indicating that sensitivity of $P2X_3R$ to ATP was not largely affected by introducing Arg^{371}-Pro^{376} sequence to its C terminus.

Cells expressing $P2X_4/X_{2a}R$ also showed a slower desensitization rate compared with the cells transfected with the wild-type $P2X_4R$ (Fig. 3*B*). The calculated time constants for the desensitization rates were 12 ± 2 ms^{-1} ($n = 12$) for $P2X_4R$ *versus* 4 ± 0.7 ms^{-1} ($n = 12$) for $P2X_4/X_{2a}R$. The averaged peak $[Ca^{2+}]_i$ amplitudes induced by 100 μM ATP were elevated in the mutant $P2X_4/X_{2a}R$ compared with wild-type $P2X_4R$ (F_{340}/F_{380}: 2.1 ± 0.1 ($n = 72$) and 1.6 ± 0.1 ($n = 55$), respectively). On the other hand, the half maximal doses of ATP required to induce maximum peak $[Ca^{2+}]_i$ response were comparable for wild-type and chimeric channels (0.8 and 1.6 μM, respectively), indicating that ATP is equipotent for both wild-type $P2X_4R$ and mutant $P2X_4/X_{2a}R$.

In further studies, the reverse mutation was performed at $P2X_{2a}R$ C terminus by substituting the Arg^{371}-Pro^{376} sequence for the corresponding 6-aa sequence of $P2X_3R$, $P2X_4R$, and $P2X_1R$, and the mutant $P2X_{2a}R$ subunits were termed $P2X_{2a}/X_3R$, $P2X_{2a}/X_4R$, and $P2X_{2a}/X_1R$, respectively. As shown in Fig. 4, traces *b, c,* and *d*, all chimeric subunits formed functional channels in GT1 cells with enhanced desensitization rates when compared with the wild-type $P2X_{2a}R$ (trace *a*). However, none of the $P2X_{2a}R$ mutants was able to mimic the rate of $P2X_{2b}R$ desensitization (trace *e*). In terms of averaged peak $[Ca^{2+}]_i$ amplitudes, no significant difference in $[Ca^{2+}]_i$ responses was observed between wild-type and mutant $P2X_{2a}R$.

TABLE I
Desensitization rate of wild-type and mutant P2XR receptors
Data shown are means ± S.E.

Receptor	Time constant
	ms^{-1}
$P2X_1R$	47 ± 6 ($n = 15$)
$P2X_{2a}/X_1R$	7 ± 0.5 ($n = 35$)[a]
$P2X_3R$	48 ± 4 ($n = 35$)
$P2X_{2a}/X_3R$	6 ± 0.6 ($n = 25$)[a]
$P2X_4R$	12 ± 2 ($n = 12$)
$P2X_{2a}/X_4R$	10 ± 0.8 ($n = 20$)

[a] $p < 0.05$ *vs.* wild-type channels.

The relevance of the 6-aa sequence in the control of desensitization in wild-type and chimeric channels are summarized in Fig. 3*C* and Table I. The rate constant for the desensitization of chimeric $P2X_4/X_{2a}R$ was indistinguishable from that of $P2X_{2a}R$ (Fig. 3*B*). Also, no significant differences were observed between $P2X_4R$ and $P2X_{2a}/X_4R$ (Table I), indicating that the structural element responsible for the distinct pattern of $P2X_{2a}R$ and $P2X_4R$ desensitization is localized to the region of the 6-aa C-terminal sequence. In contrast, the desensitization rates of $P2X_{2a}/X_1R$ and $P2X_{2a}/X_3R$ were significantly enhanced by mutations but not enough to reproduce responses seen in cells expressing wild-type $P2X_1R$ and $P2X_3R$ (Table I). Similarly, the desensitization rate of $P2X_3/X_{2a}R$ was considerably reduced, but not to the level seen in cells expressing wild-type $P2X_{2a}R$. Therefore, a part of the subunit molecule other than the C terminus also participates in the control of $P2X_1R$ and $P2X_3R$ desensitization. This agrees with literature data (13) suggesting that the transmembrane domains are critical for the fast desensitization process of $P2X_1R$ and $P2X_3R$ signaling.

We have also analyzed the relevance of $P2X_7R$ C-terminal 6-aa sequence on receptor desensitization. The optimized results of the amino acid sequence alignments for P2XRs revealed that Val^{392}-Pro^{397} sequence of $P2X_7R$ corresponds to the Arg^{371}-Pro^{376} sequence of $P2X_{2a}R$. However, a 18-aa stretch from Cys^{362} to Val^{379} of $P2X_7R$ is not related to any other subunit C termini. Thus, an insertion was needed in the alignment (1). Substitution of Val^{392}-Pro^{397} sequence with the corresponding Glu^{376}-Gly^{381} sequence of $P2X_4R$ generated a functional $P2X_7/X_4R$ mutant receptor, the Ca^{2+}-signaling function of which was indistinguishable from that of wild-type $P2X_7R$. This suggests that the C-terminal 6-aa sequence of $P2X_7R$ subunit is not functionally equivalent to those found in other subunits in terms of controlling receptor desensitization.

Identification of Residues Contributing to the Receptor Desensitization—The in-frame splicing of the $P2X_{2a}R$ C terminus starts at Val^{370} (indicated by an *arrow* in Fig. 1) and effectively removes three positively charged residues from the Arg^{371}-Pro^{376} sequence. On the other hand, negatively charged residue(s) were found in the corresponding segment of $P2X_1R$, $P2X_3R$, $P2X_{2b}R$, and $P2X_4R$ (Fig. 1), and all these receptors apparently showed faster desensitization than $P2X_{2a}R$. Such a structural difference raised the possibility that charged residues in this region may play an important role in P2XR desensitization. This is especially relevant for $P2X_{2a}/X_4R$ and $P2X_4/X_{2a}R$ mutants, whose desensitization patterns were indistinguishable from the wild type $P2X_4R$ and $P2X_{2a}R$, respectively.

To test this, we next evaluated the effects of single amino acid substitution in the $P2X_4R$ C terminus on the pattern of ATP-induced $[Ca^{2+}]_i$ response. The negatively charged residues in the 6-aa sequence of $P2X_4R$ were replaced with neutral ones, or the basic residues of the Arg^{371}-Pro^{376} sequence were introduced. As shown on Fig. 5, both elimination of negatively

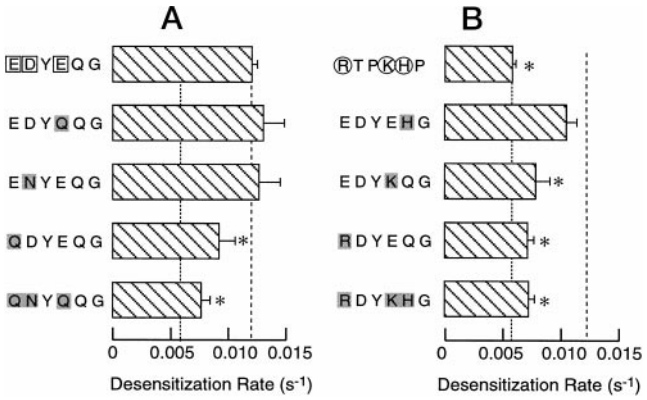

FIG. 5. **Desensitization rates of wild-type P2X$_4$R and its mutant receptors expressed in GT1 cells.** *A*, negatively charged residues of wild-type P2X$_4$R (indicated by *squares*) were substituted with neutral residues (indicated by *shading*). *B*, the positively charged residues of P2X$_{2a}$R (indicated by *circles* on *top bar*) were introduced to P2X$_4$R (indicated by *shading*). The *bars* shown are mean ± S.E. for at least 20 recordings. The *top left bar* and *dashed lines* indicate the rate of wild-type P2X$_4$R desensitization, whereas the *top right bar* and *dotted lines* indicate mean values for wild-type P2X$_{2a}$R desensitization. *Asterisks* indicate a significant difference compared with P2X$_4$R, $p < 0.05$ or higher.

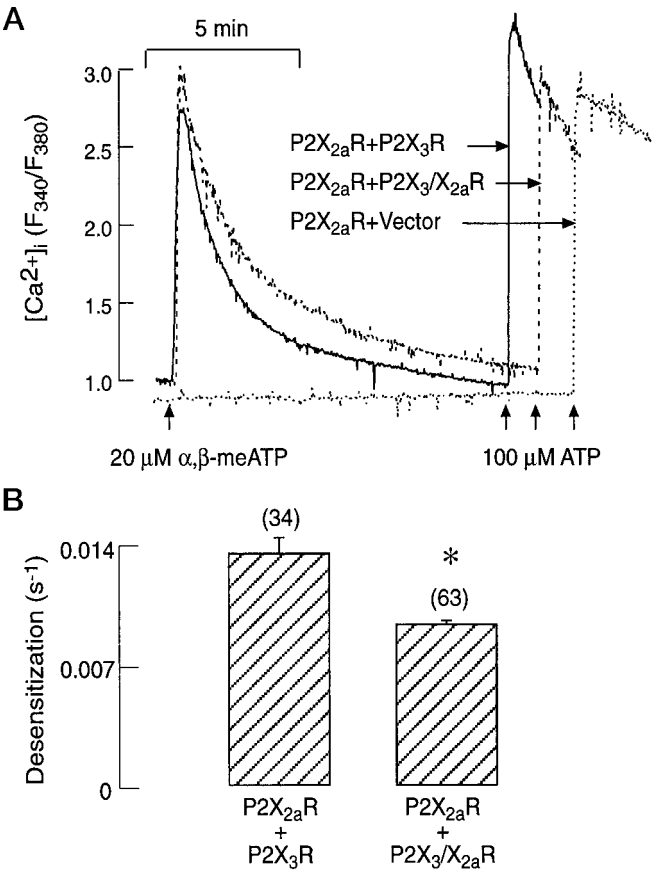

FIG. 6. **Calcium signaling in GT1 cells expressing heteropolymeric P2XRs.** *A*, pattern of $[Ca^{2+}]_i$ signaling in cells co-transfected with P2X$_{2a}$R + vector, P2X$_{2a}$R + P2X$_3$R, or P2X$_{2a}$R + P2X$_3$/X$_{2a}$R. In chimeric subunit P2X$_3$/X$_{2a}$R, the Thr^{362}-Lys^{367} sequence of P2X$_3$R was substituted with Arg^{371}-Pro^{376} sequence of P2X$_{2a}$R. The *tracings* shown are representative from 50–80 records obtained in three independent experiments. ATP was added in cultures already containing AMP-CPP (*α,β-MeATP*). *B*, desensitization rates of heteropolymeric receptors, calculated from experiments with cells stimulated with 20 μM AMP-CPP. *Bars* shown are means ± S.E., and the *asterisk* indicates a significant difference ($p < 0.05$) between means.

charged residues from and introduction of positively charged residue to the position of Glu^{376} in P2X$_4$R decreased the rate of desensitization. Mutation of Glu^{379} to a basic lysine residue also resulted in a significant decrease in the rate of desensitization. However, the point mutations at Glu^{376} or Glu^{379} could not produce the same extent of desensitization as seen in cells expressing wild-type P2X$_{2a}$R and mutant P2X$_4$/X$_{2a}$R. In addition, we constructed two mutant P2X$_4$R subunits having 3-aa substitutions, with native acidic moieties of P2X$_4$R changed to neutral (P2X4E376Q/D377Q/E379Q) or three basic amino acids of P2X$_{2a}$R introduced at the corresponding sites of P2X$_4$R (P2X4RE376R/E379K/Q380H). Both triple mutants desensitized slower than the wild-type P2X$_4$R (Fig. 5). Thus, changing the amino acid composition and the net charge of this particular C-terminal segment altered the duration of Ca^{2+} influx induced by P2X$_4$R.

Within the Arg^{371}-Pro^{376} of P2X$_{2a}$R, Thr^{372} represents an optimum phosphorylation site, (R/K)*XX*(T/S), for the type II calcium/calmodulin-dependent protein kinase (23). At the analogous position of Thr^{372}, either glutamate or aspartate was found in P2X$_1$R, P2X$_3$R, P2X$_{2b}$R, and P2X$_4$R (Fig. 1). We speculated that phosphorylation of the single Thr^{372} residue or introduction of a negatively charged moiety at this position may change the desensitization rate of P2X$_{2a}$R. However, substitution of this residue with glutamate or with glutamine did not affect the desensitization rate of mutant channels compared with that of the wild type. The desensitization constants for glutamate- and glutamine-containing mutants were 4 ± 0.3 ms^{-1} ($n = 35$) and 5 ± 0.3 ms^{-1} ($n = 21$), respectively, and 4 ± 0.2 ms^{-1} ($n = 26$) for wild-type channels. Also, no obvious difference was observed in the maximum amplitude of $[Ca^{2+}]_i$ response and the EC_{50} values for ATP between P2X$_{2a}$R and each C-terminal mutant receptors examined (not shown).

Desensitization Pattern of Heteropolymeric P2XRs—The co-expression of P2X$_{2a}$R and P2X$_3$R has been shown to form a heteropolymeric P2XR channel, which exhibits a distinct pharmacological profile and desensitization pattern from those seen in homopolymeric channels (11, 12). We used this particular subunit combination to analyze the impact of the C-terminal structure on the $[Ca^{2+}]_i$-signaling pattern of heteropolymeric channels. GT1 neurons expressing only P2X$_3$R responded to 20 μM AMP-CPP with a rise in $[Ca^{2+}]_i$, the amplitude and desensitization rate of which were highly comparable with that observed in 100 μM ATP-stimulated cells (Fig. 2). When co-expressed, these two subunits generated a channel that also responded to 20 μM AMP-CPP but with the amplitude of response comparable with that observed in homopolymeric P2X$_{2a}$R stimulated with 100 μM ATP (Fig. 6*A*). In contrast, cells co-transfected with an empty vector and cDNA for P2X$_{2a}$R did not respond to this agonist (Fig. 6*A*).

Under the continuous presence of AMP-CPP, the subsequent application of 100 μM ATP further increased $[Ca^{2+}]_i$, suggesting the existence of two channels with distinct pharmacological features in a co-transfected cell: AMP-CPP-sensitive and -insensitive (Fig. 6*A*). When the co-transfected cells were initially stimulated with 100 μM ATP, the subsequent addition of 100 μM AMP-CPP failed to induce any change in $[Ca^{2+}]_i$ (not shown). Therefore, all P2XRs-expressed cells were sensitive to ATP and desensitized completely during the initial stimulation. This suggests that the AMP-CPP-mediated rise in $[Ca^{2+}]_i$ was initiated by the activation of heteropolymeric P2X$_{2a}$R + P2X$_3$R, which desensitized more rapidly than the homopolymeric P2X$_{2a}$R but slowly when compared with P2X$_3$R (Figs. 2 and 6).

The co-expression of the P2X$_{2a}$R and C-terminal mutant P2X$_3$/X$_{2a}$R also resulted in the formation of AMP-CPP-sensitive heteropolymeric channels (Fig. 6). However, the desensiti-

zation of $[Ca^{2+}]_i$ signals generated by these channels was significantly slower than in $P2X_{2a}R$ + $P2X_3R$-expressing cells (9.5 ± 0.3 (n = 63) *versus* 13.5 ± 0.9 (n = 34), respectively). These results indicate that the C-terminal structure of the participating subunits influences the desensitization of heteropolymeric $P2X_{2a}R$ + $P2X_3R$ channels in a manner comparable with that observed in homopolymeric channels. It is also important to stress that the exact subunit stoichometry of the heteropolymeric $P2X_{2a}R$ + $P2X_3R$ and $P2X_{2a}R$ + $P2X_3/X_{2a}R$ in our experiments is not known and might vary within the cells. To overcome the possible impact of such heterogeneity on conclusions driven from these experiments, the number of recordings from which means were derived was elevated compared with other experiments (see above).

DISCUSSSION

In this study, we employed GT1 neurons as an expression system to analyze the impact of receptor desensitization on the Ca^{2+}-signaling function of recombinant P2XRs and to identify the role of C terminus in receptor desensitization. The time scale for $[Ca^{2+}]_i$ measurements in our experiments was set to be sufficiently long (5–10 min) to incorporate the consequence of a pore dilation effect during ATP stimulation reported by others (24, 25) on Ca^{2+} signaling. Under such recording conditions, activation of all homopolymeric P2XR by ATP caused a rise in $[Ca^{2+}]_i$, the pattern of which was highly specific for each particular channel. Receptors differed among themselves with respect to the amplitude of Ca^{2+} response. $[Ca^{2+}]_i$ signals initiated by the homopolymeric P2XRs also desensitized with rates characteristic to each receptor subtype: $P2X_1R$ = $P2X_3R$ > $P2X_{2b}R$ > $P2X_4R$ > $P2X_{2a}R$ > $P2X_7R$.

The kinetics of receptor desensitization estimated in single cell $[Ca^{2+}]_i$ measurements should be interpreted with two reservations. First, voltage-gated calcium channels, which are expressed by GT1 cells (18), were not silenced during $[Ca^{2+}]_i$ recording. Second, although the rank orders for receptor desensitization estimated in current and $[Ca^{2+}]_i$ measurements were highly comparable, the time needed to reach the steady desensitized states for P2XRs was significantly longer when estimated in $[Ca^{2+}]_i$ measurements (22). This probably reflects the slow kinetics of Ca^{2+} elimination from the cytoplasm, which was additionally enhanced by the integration of voltage-gated Ca^{2+} influx during receptor stimulation. Thus, $[Ca^{2+}]_i$ recordings are of limited use for studies on the dynamics of channel behavior, and the calculated rates should be interpreted only as a relative indicator of the status of receptor desensitization, especially when compared with results obtained in electrophysiological measurements.

However, we previously found a marked and comparable difference in the desensitization rates of $P2X_{2a}R$ and spliced $P2X_{2b}R$ in both current recordings and single cell $[Ca^{2+}]_i$ measurements, the later done under conditions where voltage-gated calcium channels were silent (16). In addition, the amplitudes of $[Ca^{2+}]_i$ response induced by these channels were significantly reduced when Ca^{2+} influx through L-type Ca^{2+} channels was blocked by nifedipine, but the estimated rate of receptor desensitization was not affected (17). Finally, the rank order of receptor desensitization estimated in $[Ca^{2+}]_i$ measurements was highly comparable to those observed by others in current measurements for $P2X_1R$, $P2X_3R$, $P2X_{2a}R$, $P2X_{2b}R$, and $P2X_7R$ (22).

In our experimental conditions, the rapidly desensitizing $P2X_1R$ and $P2X_3R$ were unable to induce a measurable increase in $[Ca^{2+}]_i$ when GT1 cells were bathed in physiological solution, but the inclusion of apyrase in extracellular space recovered receptors from the desensitized state. This suggests that the spontaneous release or pathological leakage of cellular ATP may prevent the fast-desensitizing receptors from responding to ATP stimulation with an increase in $[Ca^{2+}]_i$. $P2X_4R$ exhibited fast desensitization when expressed in oocytes and slow desensitization when expressed in HEK293 cells (19, 26, 27), indicating that experimental conditions, including a difference in amphibian and mammalian expression systems, may change the recombinant channel behavior (24). In our expression system, $P2X_4R$ completely desensitized during continuous agonist stimulation. With respect to the rate of desensitization, this channel should be considered as a relatively slow desensitizing one.

These observations support the validity of $[Ca^{2+}]_i$ measurements as an indicator of P2X receptor desensitization. Since the pattern of $[Ca^{2+}]_i$ response initiated by P2XRs represents signals that encode the activity of these receptors for controlling cellular functions, the time course for desensitization estimated by single cell $[Ca^{2+}]_i$ measurements is highly relevant. Also, activation of voltage-gated Ca^{2+} influx is a physiological mechanism by which P2XRs amplify $[Ca^{2+}]_i$ signals in excitable cells in addition to conducting Ca^{2+} through their pores. All together, these results indicates that selective expression of P2XR subunits in an excitable cell can serve as an effective mechanism for generating specific Ca^{2+} signals.

Our results further indicate that the variable subunit C termini in part accounts for the observed differences in the desensitization of channels. The structural element controlling the desensitization pattern of $P2X_{2a}R$ and $P2X_4R$ appears to be exclusively localized to the 6-aa C-terminal sequence. Within the Arg^{371}-Pro^{376} of $P2X_{2a}R$, Thr^{372} represents an optimum phosphorylation site, (R/K)*XX*(T/S), for type II calcium/calmodulin-dependent protein kinase and is not present in P2X4R. Nonetheless, this residue is not responsible for the difference in the desensitization of these two channels, as documented in experiments with single amino acid mutations.

It is likely that total net charge in the Arg^{371}-Pro^{376} sequence of $P2X_{2a}R$ and in the equivalent sequences of $P2X_3R$, and $P2X_4R$ is an important determinant of the extent of Ca^{2+} influx during sustained ATP stimulation. In a case of mutant $P2X_{2a}R/X_4R$, the replacement of three positive net charges with three negative ones in the equivalent segment increased the rate of desensitization compared with $P2X_{2a}/X_1R$ or $P2X_{2a}/X_3R$ mutant receptors with two and one negative residue, respectively. The relevance of single mutations at the charged residues to $P2X_4R$ desensitization was also confirmed. Both removal of negatively charged residues and introduction of positive ones resulted in a significant delay of desensitization. Furthermore, the individual residues in the 6-aa sequence of the $P2X_4R$ C terminus were not exactly equivalent in terms of their effects on receptor desensitization. Substitution of amino acids closer to the second transmembrane domain had a more profound impact on the pattern of $[Ca^{2+}]_i$ response. This domain is suggested to form a pore-lining region of P2XR (3). Since the 6-aa region of P2XR C termini is located relatively close to the cytoplasmic mouth of the pore, we may speculate that the electrical charge in the 6-aa region has an influence on the overall efficiency of conformational transition to the desensitized state.

In parallel to electrophysiological measurements (11, 12), $[Ca^{2+}]_i$ measurements showed that heteropolymerization of $P2X_{2a}R$ and $P2X_3R$ results in a channel sensitive to AMP-CPP, which desensitizes with a pattern different from those seen in cells expressing homopolymeric channels. The contribution of each subunit C terminus to $[Ca^{2+}]_i$-signaling profile was additive in this combination of subunits. Furthermore, desensitization of the heteropolymeric channels composed of $P2X_{2a}R$ and $P2X_3R$ subunit was delayed by the C-terminal mutation intro-

duced only in the $P2X_3R$ subunit. Based on the putative pseudosymmetrical orientation of the channel subunits, heteropolymeric $P2X_{2a}R$ + $P2X_3R$ could have the 6-aa C-terminal region of each subunit at an equivalent position around the pore axis. Such a ring-like structure made by the C-terminal-charged residues could determine the pattern of P2XR signaling.

In contrast to the other receptor subunits, mutation at the C-terminal 6-aa sequence of $P2X_7R$ did not result in modulation of receptor desensitization. This is not a surprise, since the structure of $P2X_7R$ C terminus is distantly related to others. It is the longest C terminus among P2XRs and contains the structural basis underlying the unique feature of this channel, the cell-lytic pore formation. It also shows the least amino acid sequence similarity compared with the other P2XR C termini (10). The amino acid sequence alignment of P2XRs revealed that an 18-aa stretch of $P2X_{7R}$, with no similarity to others, is positioned proximal to the Val^{392}-Pro^{397} sequence, which corresponds to the Arg^{371}-Pro^{376} sequence of $P2X_{2a}R$ (1). This insertion should effectively move the charged 6-aa residues away from the internal mouth of the pore.

A role of the C terminus in receptor signaling is not unique for P2XRs. The contribution of the C terminus to channel gating was reported for other channels, including acetylcholine-gated channels, inward rectifier potassium channels, and mechano-sensitive channels (28–31). In the case of inwardly rectifying potassium channels, which have the same topological architecture as P2XRs, the important determinants of the pore block by Mg^{2+} and polyamines are mediated by negatively charged residues located in the C terminus and the second transmembrane region (29). The mechanism for P2XR desensitization by the charged C-terminal small segment needs to be further examined by means of structural and biophysical studies.

In conclusion, we show here that the activation of P2XRs by ATP leads to an increase in $[Ca^{2+}]_i$, the pattern of which is highly specific for each channel expressed and determined by the rate of receptor desensitization. The variable C termini of receptor subunits in part account for the observed difference in desensitization rates of homo- and heteropolymeric receptors. The charged residues in the 6-aa C-terminal sequence appear to serve as a common factor influencing the desensitization rates of $P2X_3R$, $P2X_{2a}R$, $P2X_{2b}R$, and $P2X_4R$. The structural element responsible for the difference in desensitization rates among $P2X_{2a}R$, $P2X_{2b}R$, and $P2X_4R$ is exclusively localized to the 6-aa C-terminal sequence. In the case of $P2X_1R$ and $P2X_3R$ subunits, the structure other than the C termini also participates in the control of desensitization. Finally, $P2X_7R$ has a distinct C terminus, as well as a distinct pattern of $[Ca^{2+}]_i$ signaling, and further experiments are required to establish the possible relationship between the structure of this terminus and the sustained Ca^{2+} influx.

REFERENCES

1. Buell, G., Collo, G. & Rassendren, F. (1996) *Eur. J. Neurosci.* **8,** 2221–2228
2. North, R. A. (1996) *Neurosciences* **8,** 187–194
3. Ralevic, V. & Burnstock, G. (1998) *Pharmacol. Rev.* **50,** 413–492
4. Valera, S., Hussy, N., Evans, R. J., Adami, N., North, R. A., Surprenant, A. & Buell, G. (1994) *Nature* **371,** 516–519
5. Brake, A. J., Wagenbach, M. J. & Julius, D. (1994) *Nature* **371,** 519–523
6. Chen, C.-C., Akoplan, A. N., Sivllott, L., Colquhoun, D., Burnstock, G. & Wood, J. N. (1995) *Nature* **377,** 428–431
7. Bo, X., Zhang, Y., Nassar, M., Burnstock, G. & Schoepfer, R. (1995) *FEBS Lett.* **375,** 129–133
8. Garcia-Guzman, M., Soto, F., Laube, B. & Stuhmer, W. (1996) *FEBS Lett.* **338,** 123–127
9. Collo, G., North, R. A., Kawashima, E., Merlo-Pich, E., Neidhart, S., Surprenant, A. & Buell, G. (1996) *J. Neurosci.* **16,** 2495–2507
10. Surprenant, A., Rassendren, F., Kawashima, E., North, R. A. & Buell, G. (1996) *Science* **272,** 735–738
11. Lewis, C., Neidhart, S., Holy, C., North, R. A., Buell, G. & Surprenant, A. (1995) *Nature* **377,** 432–435
12. Radford, K. M., Virginio, C., Surprenant, A., North, A. & Kawashima, E. (1997) *J. Neurosci.* **17,** 6529–6533
13. Werner, P., Seward, E. P., Buell, G. N. & North, R. A. (1996) *Proc. Natl. Acad. Sci. U. S. A.* **93,** 15485–15490
14. Brandle, U., Spielmanns, P., Osteroth, R., Sim, J., Surprenant, A., Buell, G., Ruppersberg, J. P., Plinkert, P. K., Zenner, H. P. & Glowatzki, E. (1997) *FEBS Lett.* **404,** 294–298
15. Simon, J., Kidd, E. J., Smith, F. M., Chessell, I. P., Murrell-Lagnado, R., Humphrey, P. P. A. & Barnard, E. A. (1997) *Mol. Pharmacol.* **52,** 237–248
16. Koshimizu, T., Tomic, M., Van Goor, F. & Stojilkovic, S. S. (1998) *Mol. Endocrinol.* **12,** 901–913
17. Koshimizu, T., Tomic, M., Koshimizu, M. & Stojilkovic, S. S. (1998) *J. Biol. Chem.* **273,** 12853–12857
18. Van Goor, F., Krsmanovic, L. Z., Catt, K. J. & Stojilkovic, S. S. (1999) *Mol. Endocrinol.* **13,** 587–603
19. Buell, G., Lewis, C., Collo, G., North, R. A. & Surprenant, A. (1996) *EMBO J.* **15,** 55–62
20. Kozak, M. (1991) *J. Cell Biol.* **115,** 887–903
21. Horton, R. M., Hunt, H. D., Ho, S. N., Pullen, J. K. & Pease, L. R. (1989) *Gene* **77,** 61–68
22. Evans, R. J., Surprenant, A. & North, R. A. (1997) *The P2 Nucleotide Receptors* (Turner, J. T., Weisman, G. A., and Fedan, J. S., eds) pp. 43–61, Humana Press Inc., Totowa, NJ
23. Pearson, R. B. & Kemp, B. E. (1991) *Methods Enzymol.* **200,** 62–81
24. Khakh, B. S., Bao, X. R., Labarca, C. & Lester, H. A. (1999) **2,** 322–330
25. Virginio, C., MacKenzie, A., Rassendren, F. A., North, R. A. & Surprenant (1999) *Nat. Neurosci.* **2,** 315–321
26. Soto, F., Garcia-Guzman, M., Gomez-Hernandez, J. M., Hollmann, M., Karschin, C. & Stuhmer, W. (1996) *Proc. Natl. Acad. Sci. U. S. A.* **93,** 3684–3688
27. Seguela, P., Haghighi, A., Soghomonian, J. & Cooper, E. (1996) *J. Neurosci.* **16,** 448–455
28. Yang, J., Jan, Y. N. & Jan, L. Y. (1995) *Neuron* **15,** 1047–1054
29. Pessia, M., Bond, C. T., Kavanaugh, M. P. & Adelman, J. P. (1995) *Neuron* **14,** 1039–1045
30. Corringer, P. J., Bertrand, S., Galzi, J. L., Devillers-Thiery, A., Changeux, J. P. & Bertrand, D. (1999) *Neuron* **22,** 831–843
31. Chang, G., Spencer, R. H., Lee, A. T., Barclay, M. T. & Rees, D. C. (1998) *Science* **282,** 2220–2226